THE IMPACT OF CAPILLARY INSTABILITY AND FURNACE OPERATING CONDITIONS ON THE FABRICATION OF DRAWN METAMATERIALS

Xue S.C * [1], Barton G.W [1], Fleming S. [2] and Argyros A. [2]
*Author for correspondence
[1]: School of Chemical and Biomolecular Engineering
[2]: Institute of Photonics and Optical Sciences (IPOS), School of Physics
The University of Sydney,
NSW 2006
Australia,
E-mail: shicheng.xue@sydney.edu.au

ABSTRACT

Metamaterials are composites containing metal structures imbedded within a dielectric matrix. Their nanoscale structure gives them optical properties that don't exist in naturally occurring materials. This paper focuses on the issue of Plateau-Rayleigh instability when fibre drawing technology is used to manufacture such metamaterials. Linear stability analysis can identify the key operating parameters that influence the instability of the metal core as a function of the metal/dielectric combination used in the drawn fibre. To verify these theoretical predictions, a numerical fibre drawing model, developed using commercially available software, is used to examine the non-isothermal drawing of a polymer preform containing a concentric metal core in a cylindrical furnace. All heat transfer modes are included. To determine the external radiative heat flux across the preform surface, a Monte Carlo Ray-Tracing method is coupled with the drawing model to calculate the view factors between the furnace walls and the deforming preform. The impact of the key operating parameters on the drawing instability is numerically investigated with a simplified version of this heat transfer model. Optimized operating conditions that minimize drawing instability are proposed.

INTRODUCTION

Metamaterials are an 'artificial' class of composites that contain a metallic grid structure embedded within a dielectric matrix. Such composites, engineered on the nanoscale, can give properties unavailable in nature [1-2].

The concept of metamaterials has been discussed for over a decade [3]. However, fabricating highly regular composites of dissimilar materials on the scale required presents challenges, especially for those processes that can be scaled-up to produce commercial quantities in a cost-effective manner.

Recently, fibre drawing techniques used in the high-volume fabrication of various optical fibres have been adapted to the creation of metamaterials [4]. Figure 1 shows a preform being fed into a furnace and continuously drawn down to fibre under an applied tension. Drawing has the significant advantage over most other micro-fabrication techniques in that the desired structure is created in a macro-scale preform that is then drawn down many orders of magnitude. In drawing a metamaterial, the preform is fabricated either by milling and metal insertion or by stacking together multiple metal-filled capillaries.

NOMENCLATURE

A	[m]	amplitude
h	[J/m^{2}Ks]	heat transfer coefficient
H	[m]	furnace height
k	[1/m]	frequency
L	[m]	neck-down length
n		local normal to the surface
q	[W/m^2]	heat flux
R, r	[m]	radius
T	[K]	temperature
T_g	[K]	glass transition temperature
t	[s]	time
v	[m/s]	axial velocity
V	[m/s]	velocity
z	[m]	axial position

Special characters

ε		hemispherical emissivity
γ	[N/m^2]	interfacial surface tension between the core surface and the cladding inner surface
κ	[W/mK]	thermal conductivity
λ	[m]	wavelength
μ	[Pa.s]	viscosity
σ_0		Stefan-Boltzmann constant (5.68×10^{-8} W/m^2 K^4)

Subscripts

a	hot air surrounding preform surface
e	equivalent
f	fibre drawing
i	initial or feeding
k	element
m	metal
max	maximum value
0	initial
p	polymer or preform
r	radiative
w	furnace wall

Microscale drawn metamaterials with a complex internal structure formed by a low melting point metal (indium) imbedded in a polymer (polymethylmethacrylate or PMMA) matrix have been fabricated [5]. Such metamaterials operate in the THz and mid-IR wavelengths. However, to operate in the

optical wavelengths requires metamaterial structures at least an order of magnitude smaller. Fabricating such metamaterials by drawing could face a major challenge due to Plateau-Rayleigh instability which describes the tendency of a cylindrical liquid thread, contained within another fluid, to break up into a stream of spherical droplets due to surface tension effects.

From linear instability analysis [6-7], it is known that the growth rate of surface perturbations on the inner metal core is both scale and physical property dependent; the key parameters being the core radius, the interfacial surface tension between the two materials as well as their viscosities. Thus, core instability is affected by furnace operating conditions, notably the shape and temperature profiles in the neck-down region, both of which are affected by the furnace temperature as well as the feed rate of the preform.

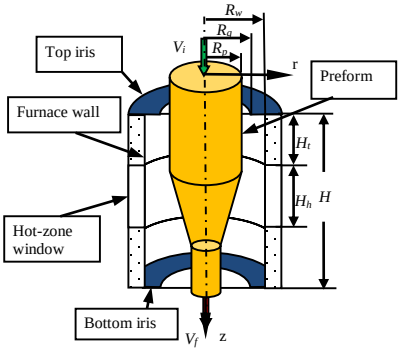

Figure 1 Geometrical configuration for the drawing process.

Experimental data from drawing a PMMA preform with an indium core has shown the increasing importance of this mode of instability as the scale of the drawn fibre was progressively reduced [8] due to the metal core breaking up into droplets.

In an attempt to guide future experimental campaigns, the present study explored this instability mode via analysis of the fibre drawing process. A commercially available finite element method based solver, ANSYS PolyFlow [9], is used to establish an efficient numerical model able to simulate the non-isothermal drawing of a polymer/metal capillary.

FACTORS AFFECTING CAPILLARY INSTABILITY

Consider a viscous cylindrical liquid column (of viscosity μ_m) embedded in a viscous cladding (of viscosity μ_p) where the system is experiencing a periodic perturbation (with spatial frequency k and initial amplitude A_0) along its length L. If the column is thin enough, the system is unstable and the column will breakup into liquid droplets so as to minimize the surface energy. The development of this column breakup process can be described in terms of the growth of the amplitude of the periodic perturbation.

In a fibre drawing process, the preform is progressively scaled down to thin fibre over the length L of the neck-down region. The growth of the accumulated (or integral) amplitude A over this region can be used as an indicator of likely development of any instability. In a recent work [7] based on Tomotika's seminal work [6], the factors that contribute to the behaviour of A when drawing a metamaterial for the case where $\mu_m / \mu_p \to 0$ (noting that for a PMMA/indium preform, this condition is satisfied as $\mu_m / \mu_p = 10^{-8}$) were identified in terms of two localized dimensionless numbers, i.e. the aspect ratio $\delta(\mathrm{Z}) = r(\mathrm{Z})/L$ and the capillary number $C_a(\mathrm{Z}) = v\mu_p(\mathrm{Z})/\gamma$:

$$A = A_0 \mathrm{e}^{\Gamma}, \tag{1}$$

where

$$\Gamma = \frac{K(x)}{2}\int_0^1 g(\mathrm{Z})\mathrm{dZ}, \tag{2}$$

is referred to as the total growth where $x = 2\pi r/\lambda$ and $K(x) = (1-x^2)\Phi(x)$ with $\Phi(x)$ being a known function (see [6] for details). The axial position dependent integrand:

$$g(\mathrm{Z}) = \frac{1}{\delta(\mathrm{Z})C_a(\mathrm{Z})} > 0, \tag{3}$$

is the instability growth factor where the axial position z has been scaled by L (i.e., $Z = z/L$). Because $K(x)$ decreases linearly from its maximum value (~1) to 0 as x increases from 0 to 1, for a given most unstable wavelength, the magnitude of Γ is determined by $g(Z)$.

Due to the dependence of the two dimensionless numbers on Z, $g(Z)$ can only be obtained numerically, although qualitatively the impact of the furnace operating conditions on the instability of the drawing process can be identified from this relationship. For example, a lower cladding viscosity will lead to a larger growth factor, while for a given cladding viscosity and core size, a short deformation zone will stabilize the process.

As demonstrated in our previous work [7], under isothermal conditions, if the necking preform can be characterized as a 'slender body' (i.e. if $\delta(0) << 1$), then the total growth term can be approximated as:

$$\Gamma \approx \frac{K(x)}{\alpha\delta(0)C_a(0)}\sum_1^n \frac{\psi^{k-1}}{k}, \tag{4}$$

where $\alpha = \ln D_r$ with the draw ratio $D_r = \mathrm{V_i/V_f}$ and

$$\psi = \left(\frac{R(0)}{r(0)}\right)\left(\frac{1}{\alpha\delta(0)C_a(0)}\right) < 1. \tag{5}$$

Because ψ is non-zero, some level of instability is thus unavoidable. However, it can be minimized if the combination of metamaterial structure, materials and operating conditions are judiciously selected. Thus, a large core size relative to the preform, a higher draw ratio (i.e. a faster draw), a large aspect ratio (i.e. a short neckdown region), and a large capillary number (i.e. a small interfacial surface tension, coupled with a fast/cold draw) will each contribute to minimizing instability.

In order to confirm/quantify these theoretical predictions, numerical modelling simulations were next carried out of the non-isothermal fibre drawing process.

A VALIDATED CONJUGATE FLOW AND THERMAL MODEL OF DRAWING FURNACE

In our previous drawing work using PolyFlow, a single-phase model was employed for the non-isothermal drawing of an annular hollow fibre [10]. There, however, only convective heat transfer at the preform surface was considered. Radiative heat

transfer between the furnace walls and the preform surface was not taken into account; such a simplification becoming increasingly invalid with an increased furnace operating temperature.

To provide a more realistic model for the present study, the process was treated as a fully conjugate two-phase system [11], involving both the preform and the surrounding hot air as bounded by the furnace. At the interface (i.e. preform surface), the hot air is considered as a non-participating medium with net heat flux continuity applied:

$$-\kappa\frac{\partial T}{\partial n}\bigg|_a - q_r = \kappa\frac{\partial T}{\partial n}\bigg|_p , \qquad (6)$$

where the net heat flux q_r at the preform surface due to radiative transfer is determined by using the net-radiation method [12-13] to the entire furnace enclosure by discretising each surface into either ring elements (for the preform and the vertical walls of the furnace) or annular disk elements (for the top and bottom iris surfaces). Element sizes (i.e. height for the ring elements; width for the annular disk elements) were small enough so that the temperature of each can be considered as constant. For element k ($1 \le k \le N$ with N being the total number of elements in the entire enclosure), the net heat flux was cast as having the same form as that for two infinitely long concentric cylinders:

$$q_{r,k} = \varepsilon_k \sigma_0 \left(T_k^4 - T_{e,k}^4\right) \qquad (7)$$

where $T_{e,k}$ is a local 'equivalent radiative heating temperature' obtained from the net-radiation method.

This multiphase model was validated by matching the predicted temperature profiles along the preform centreline and surface with experimentally measured profiles obtained from a run without preform deformation. Using this validated model, a meaningful neck-down (i.e. preform to fibre) shape is expected as this shape is largely determined by the axial temperature profile along the deforming preform.

However, to numerically predict the neck-down shape in cases where external radiative heat transfer is included, one needs to account for severely deformed free surfaces, which is still a challenging issue in computational fluid dynamics, as well as accurately determining the view factors F_{k-j} between each pair of elements ($1 \le j \le N$) within the drawing furnace.

In this work, Monte Carlo Ray-Tracing (MCRT) techniques [14] were used within a generic software package to determine view factors in any three-dimensional configuration [15]. This code has been optimised to exploit the high-speed graphical processing units found in modern computers.

As view factors change once the preform starts necking, the MCRT code was interfaced to the PolyFlow package, and an iteration solution procedure employed to update both the preform shape and temperature field:

1. In PolyFlow, starting with a cylindrical preform and treating the system as two infinitely long concentric cylinders with the measured wall temperature profile (T_w) taken as the radiative heating temperature, initial profiles for the preform shape and temperature are predicted;
2. Based on the latest preform shape, calculate the view factors F_{k-j} via the MCRT code and thus obtain $T_{e'k}$;
3. In PolyFlow, $T_{e'k}$ is used as the equivalent radiative heating temperature for the external radiative heat transfer (see Eq.(7)), and the preform shape and temperature field are recalculated.
4. Repeat Steps 2 and 3 until the profiles for the preform shape and temperature field have converged.

For all cases examined, this procedure converged to an acceptable accuracy within no more than two iterations.

With this multiphase model, however, there were numerical divergence issue, especially at high draw ratio (D_r) values, despite exploiting one of PolyFlow's most attractive features, that is, a robust ability to relocate internal nodes based on the displacement of nodes along free surfaces so as to update the shape of a free surface without the need to remesh the whole system.

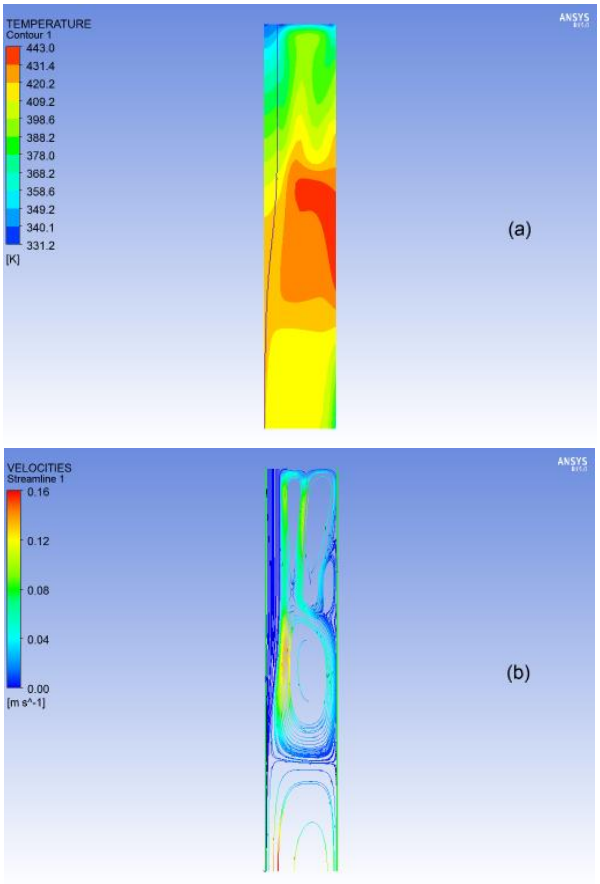

Figure 2 Temperature contours and streamlines in (a) the preform, and (b) the surrounding hot air.

Indeed, when this multiphase model was used to carry out fibre drawing simulations under various operating conditions (by varying the controllable parameters including the preform radius R_p, the preform feed rate V_i, the draw ratio D_r, and the furnace heating temperature at the set-point T_{set}), at high D_r values, in most cases no convergent solution was reached despite employing a range of strategies within PolyFlow to enhance numerical stability. The primary reason behind this numerical divergence is felt to be the extreme difference in the spatial dimensions of phases in the system. With the furnace radius and length being fixed at 32 mm and 180 mm, respectively, if the

metal core radius in the final fibre is 10^{-3} mm, then the dimensionless size in the radial direction will range from 3.2×10^{-4} to 1, which would require severe deformations in the mesh structure to the meshes that are already refined around the interfaces of the three constituent materials (i.e. the metal core, the surrounding polymer and the hot air), a situation known to cause numerical difficulties leading to divergence. In addition to these numerical issues, it became impracticable, in terms of CPU time consumptions, to run the simulations with the mesh resolution required to capture the highly complex flow pattern induced by the moving preform and the buoyant force within the hot air in the enclosed furnace.

As an example of a converged solution, the temperature contour and streamlines for drawing a solid PMMA preform of initial radius 6 mm to fibre at V_i = 6 mm/min and D_r = 533 are shown in Figure 2. In this simulation, by the fact of that, at the top iris there was no gap around the preform, while the bottom iris was wide open, an insulated surface was assumed for the top iris; the bottom iris was modelled as a black surface at the ambient temperature T_∞ of 298 *K*. Along the furnace vertical wall, the measured T_w profile (shown as the solid line in Figure 3) with the temperature at the set-point T_{set} of 473 K (a reference point towards the middle of the furnace wall where a thermocouple is attached) was approximated by linear interpolation from the measured point-wise data. The computational domain was discretised into 5400 non-uniform quadrilateral elements formed by 180 cells in the axial direction along the preform, 10 cells across the preform radius with a finer mesh used around the interface, and 20 cells for the radial space between the preform surface and the furnace wall with finer meshes again used around all boundaries and interfaces. As can be seen, the flow field of the hot air inside the furnace is very complex when drawing a fibre under these furnace heating conditions.

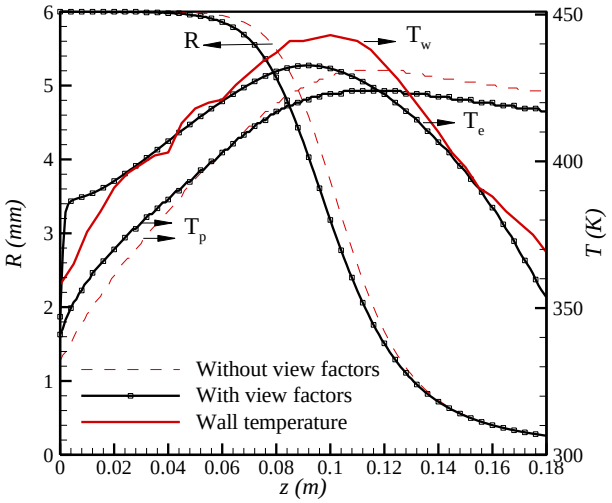

Figure 3 Axial profiles of T_w, $T_{e'k}$ and the resultant T_p and neck-down shapes when the external radiative heat transfer are included with and without evaluating view factors.

The importance of accurately calculating F_{k-j} to account for the external radiative heat transfer becomes apparent if we compare the axial profiles shown in Figure 3 for T_w (i.e. the solid line) and $T_{e'k}$ (i.e. the solid line with symbols). As can be seen, if the system is treated as two infinitely long concentric cylinders (i.e. view factors are not evaluated using the MCRT code; indicated in Figure 3 by 'without view factors'), marked difference in the resultant preform temperature and neck-down shapes (i.e. the dashed lines) are in evidence compared to the results obtained (i.e. the solid lines with symbols) after considering the influence of the neck-down shape on the external radiative heat transfer by calculating F_{k-j} with the MCRT code.

Even for PMMA based fibre drawing, the external radiative heat transfer can be significant. For glass based metamaterials, where furnace operating temperatures are significantly higher, external radiative heat transfer is expected to be the dominant heat transfer mode, and thus it would be critical to calculate the view factors accurately, while convective heat transfer at the preform surface would become less important.

MODEL SIMPLIFICATION

Due to the relative importance of radiative and convective heat transfer and the challenges in converging the multiphase model, it was decided to develop a simplified single-phase model where the external radiative heat transfer between the furnace walls and the preform surface was still calculated using F_{k-j} and $T_{e,k}$ as in the multiphase case, but the convective heat transfer between the surrounding hot air and the preform surface was determined using a realistic external heat transfer coefficient. With this simplification, not only were numerical divergence issues avoided, but significantly faster simulations resulted due to the reduced spatial difference in the computational domain and there being no need to calculate the complex flow and thermal fields in the hot air.

In this single-phase model, condition (6) becomes:

$$-h(T-T_a)-q_r=\kappa\left.\frac{\partial T}{\partial n}\right|_p \qquad (8)$$

where h and T_a have to be determined. Extensive calculations for determining suitable h and T_a values for the fibre drawing process has been undertaken [7] by matching the simulated results (in terms of predicted profiles for $R(z)$ and $T(z)$) from the single-phase model with those from the corresponding multiphase model as well as experimental measured results. It was found that empirical correlations used in fibre spinning are unsuitable for the current process; indeed, the best match obtained was to use a constant h (= 20 J/m^{2}Ks) combined with the following trapezoid-like profile for T_a:

$$T_a(z)=\begin{cases}0.85T_w(z)\ \text{or}\ T_w(0)\ \text{if}\ T_a\le T_w(0) & 0\le z<z_-\\ T_{a'\max} & z_-\le z\le z_+\\ T_w(H)+\dfrac{(T_{a'\max}-T_w(H))}{(0.9H-z_m)}(H-z) & z_+<z\le H\end{cases} \qquad (9)$$

where $z_\pm = z_m \pm 0.1H$ and $T_{a'max} = 0.85T_{w'max}$ with z_m the location of $T_{w'max}$.

Figure 4 shows the profiles of $R(z)$ and $T(z)$) predicted by the multiphase and single-phase models for the case of drawing a solid PMMA preform of initial radius R_p = 2.5mm to fibre at V_i = 2 min/mm and D_r = 2500 with the furnace T_{set} being 503 K. As can be seen, the two key parameters (i.e., $R(z)$ and $T(z)$) determining the instability behavior are essentially overlapping.

Thus, in the context of the present study, the use of a single-phase model with external radiative heat transfer considered is sufficiently accurate for undertaking instability analyses when drawing fibre based metamaterials.

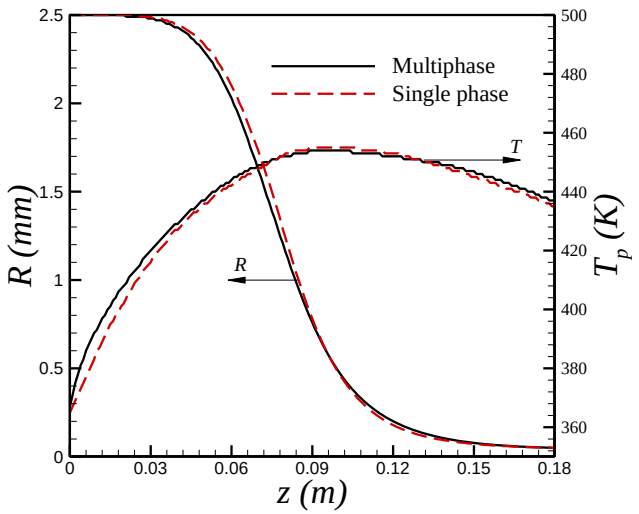

Figure 4 Predicted neck-down shapes and preform surface temperature profiles with different numerical models.

In the following section, the simplified single-phase model is used to carry out numerical simulations of the drawing of an indium-in-PMMA fibre under various operating conditions, and comparing the results to the previous analytical predictions.

COMPARISON OF ANALYTICAL AND NUMERICAL MODEL INSTABILITY PREDICTIONS

The previous theoretical analysis allows assessment of the likely impact of fibre drawing conditions on metamaterial instability; notably that for a given metamaterial, the instability growth factor is determined by the combination of a group of dimensionless numbers that can be related to the adjustable parameters R_p, V_i, T_{set}, and D_r. If the furnace is also included, then, another two 'controllable' variables become available, namely the furnace diameter and the length of the heated zone.

Using the validated numerical model of the fibre drawing process, it is possible to investigate the impact of these key controllable variables on capillary instability under different operating conditions, thus confirming the validity of the theoretical analysis and shedding light on the most appropriate furnace operating conditions to employ so as to minimize the instability in the fibre drawing. The results are shown in Figures 5 to 8.

Firstly, the impact of V_i, D_r, and T_{set} was investigated at a fixed R_p (= 2.5 mm) for an indium/PMMA capillary system with a final metal core radius of 2.5 μm.

1) Impact of preform feed rate V_i

With the other conditions fixed (D_r = 2500; T_{set} = 503 K), growth factors at two different feed rates (i.e. 2 and 6 mm/min) were calculated using the model simulation results. As shown in Figure 5, the growth factor is much higher at the lower V_i value, confirming that a 'fast draw', or higher feed rate, will reduce core instability.

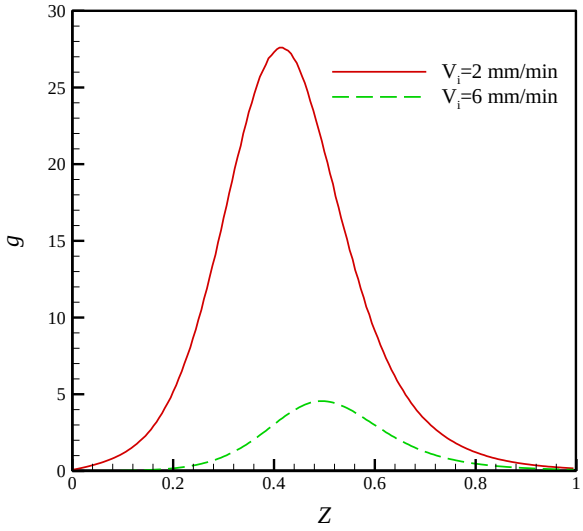

Figure 5 g(Z) at a fixed T_{set} = 503 *K* and varying V_i

2) Impact of furnace temperature (i.e. T_{set})

Growth factors at two different furnace heating temperatures (i.e. T_{set} = 473 K and 503 K), with other conditions fixed (D_r = 2500; V_i = 2 mm/min), were next calculated. Figure 6 shows that the growth factor is significantly higher for T_{set} = 503 K, confirming that a cold draw will reduce core instability.

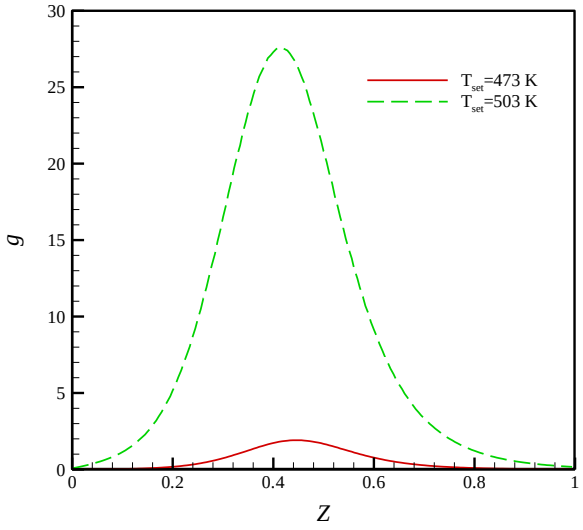

Figure 6 g(Z) at a fixed V_i = 2 mm/min and varying T_{set}

3) Impact of draw ratio D_r

Finally, growth factors at three different draw ratios (i.e. D_r = 400, 900 and 2500) were determined, with other conditions fixed (T_{set} = 473 K; V_i = 2 mm/min). Figure 7 shows that a high draw ratio corresponds to a smaller growth factor, again confirming that fast fibre drawing reduces core instability. However, the impact on instability arising from changes in D_r is less than the sensitivity brought about by changes in both V_i and T_{set}.

Based on the numerical confirmation of the previous theoretical predictions, one can conclude (i) that a fast/cold draw is more stable than a slow/hot draw, and (ii) that core instability is more sensible to variations in furnace temperature than to the drawing speed (achieved either by increasing V_i or D_r).

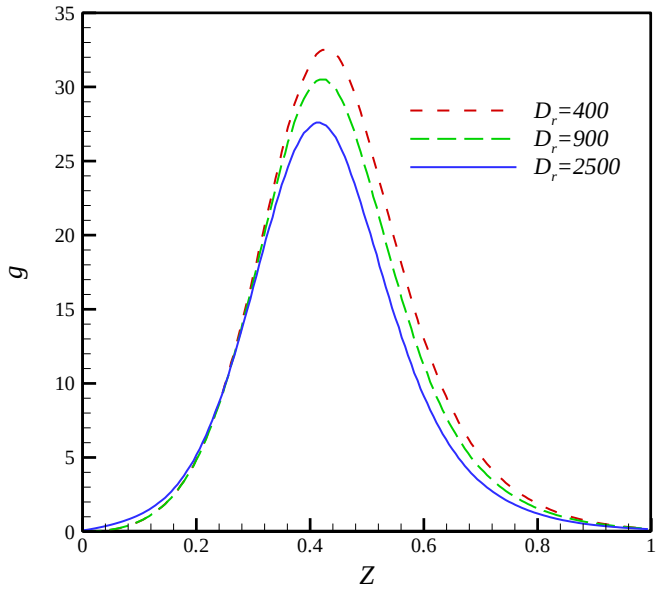

Figure 7 g(Z) at a fixed V_i (= 2 mm/min) and T_{set} (=503 K) but varying D_r

Ongoing research focuses on the application of these tools for the fabrication of a range of glass-based metamaterials.

CONCLUSIONS

Linear analysis shows that the instability of the metal core in a fibre-based metamaterial can be defined in terms of two dimensionless numbers; namely, the capillary number and the preform aspect ratio. The impact of different combinations of these dimensionless groups on drawn fibre instability has been explored, for an indium-in-polymer capillary system, using a validated numerical model of a drawing furnace. The value of such instability analysis is that it can help shed light on both the most promising metal/dielectric combinations to use in terms of fibre drawability, and the most appropriate furnace operating conditions in terms of minimizing drawing instability.

REFERENCES

[1] Wegener, M. and Linden, S.Photonic metamaterials: Optics starts walking on two feet, *Proceedings of Metamaterials 2008*, Sept 2008.

[2] Tuniz, A., Kuhlmey, B. T., Chen, P. and Fleming, S. C., Weaving the invisible thread: design of an optically invisible metamaterial fibre, *Optics Express*, Vol.18, 2010, pp.18095-18105

[3] McPhedran, R. C., Shadrivov, I.V., Kuhlmey, B.T. and Kivshar, Y.S.,Metamaterials and metaoptics, *NPG Asia Materials*, Vol.3, 2011, pp.100-108.

[4] Zhang, X., Ma, Z., Yuan, Z. Y. and Su, M., Mass-productions of vertically aligned extremely long metallic micro/nanowires using fiber drawing nanomanufacturing, *Adv. Mater.* Vol. 20, 2008, pp.1310–1314

[5] Fleming, S., Tuniz, A., Argyros A. and Kuhlmey, B., Metamaterials Fabricated by Drawing, *Invited Paper at the 2012 Conference on Lasers and Electro-Optics (CLEO)*, San Jose, USA, 6-11 May 2012.

[6] Tomotika, S., On the instability of a cylindrical thread of a viscous liquid surrounded by another viscous fluid, *Proceedings of the Royal Society of London, Series A, Mathematical and Physical Sciences*, Vol. 150, 1935, pp.322–337.

[7] Xue S.C., Barton G.W., Fleming S. and Argyros A., Theoretical and numerical analyses on capillary instability in fabrication metamaterials using fibre drawing technology, *Int. J. Heat and Mass transfer*, To be submitted, 2016.

[8] Naman, O. T., New-Tolley, M. R., Lwin, R., Tuniz, A., Al-Janabi, A. H., Karatchevtseva, I., Fleming, S. C., Kuhlmey, B. T. and Argyros, A., Indefinite Media Based on Wire Array Metamaterials for the THz and Mid-IR, *Advanced Optical Materials*, Vol.1,2013, pp. 971-977.

[9] ANSYS POLYFLOW User's Guide, Ansys Inc., 2010.

[10] Xue, S. C., Tanner, R. I., Barton G. W., Lwin, R., Large, M. C. J. and Poladian, L., Fabrication of Microstructured Optical Fibres, Part II: Numerical Modelling of Steady-State Draw Process, *J. Lightwave Technol.* Vol. 23,2005, pp.2255-2266.

[11] Xue, S.C., Barton, G.W., Tanner, R.I., Heat Transfer within a Furnace for Drawing Microstructured Optical Fibres, *Proc 18th International Conference on POF 2009*, Sydney, Australia, Sept. 9-11, 2009.

[12] Siegel, R. and Howell, J.R., Thermal Radiation Heat Transfer. Hemisphere Publishing Corporation, Washington D.C., 1992.

[13] Xue, S.C., Poladian, L., Barton, G.W., Large, M. C. J., Radiative Heat Transfer in Preforms for Microstructured Optical Fibres, *Int. J. Heat and Mass transfer*, Vol. 50, 2006, pp.1569-1579.

[14] Walker, T., Xue S.-C. and Barton, G.W., Numerical determination of radiative view factors using ray tracing, *Journal of Heat Transfer*, Vol. 132, 2010, pp. 072702-1/6.

[15] Walker, T., Xue S.-C. and Barton, G.W., A robust Monte Carlo based ray-tracing approach for the calculation of view factors in arbitrary three-dimensional geometries, *Computational Thermal Sciences*, Vol. 4, 2012, pp 425-442.